Available online at www.sciencedirect.com
ScienceDirect
Journal of Solid State Chemistry 180 (2007) 628–635
JOURNAL OF SOLID STATE CHEMISTRY
www.elsevier.com/locate/jssc

Structure and magnetism of rare-earth-substituted $Ca_3Co_2O_6$

Charles H. Hervoches[a,*], Helmer Fjellvåg[b], Arne Kjekshus[b], Vivian Miksch Fredenborg[b], Bjørn C. Hauback[a]

[a]*Institute for Energy Technology, P.O. Box 40, N-2027 Kjeller, Norway*
[b]*Centre for Materials Science and Nanotechnology; Department of Chemistry, University of Oslo, P.O. Box 1033 Blindern, N-0315 Oslo, Norway*

Received 2 August 2006; received in revised form 30 October 2006; accepted 31 October 2006
Available online 16 November 2006

Abstract

Yttrium- and rare-earth-substituted derivatives of $Ca_{3-v}R_vCo_2O_6$ (R=Y, Pr, Nd, Sm, Eu, Gd, Tb, Dy, Ho, Yb, and Lu) have been synthesized and structurally characterized by powder X-ray and neutron diffraction. All phases adopt the K_4CdCl_6-type structure with space group $R\bar{3}c$), in which the trivalent R^{3+} substituents randomly occupy the Ca^{2+} site. The homogeneity range of $Ca_{3-v}R_vCo_2O_6$ extends to $v \approx 0.90$ for the substituents concerned. A significant increase in the Co2–O distances within the trigonal-prismatic $Co2O_6$ coordination polyhedra upon introduction of R^{3+} confirms that extra electrons from the R^{3+}-for-Ca^{2+} substitution exclusively enter the Co2 site of the quasi-one-dimensional $Ca_{3-v}R_vCo_2O_6$ structure, thereby formally reducing its oxidation state. This is furthermore supported by magnetic susceptibility and low-temperature neutron diffraction measurements. The long-range ferrimagnetic ordering temperature is reduced upon R substitution and appears to vanish for $v > \sim 0.30$.

Keywords: Rare-earth substitution; $Ca_3Co_2O_6$ structure; Low-dimensional material; Magnetic properties

1. Introduction

Low-dimensional magnetic materials have attracted considerable interest in recent years. $Ca_3Co_2O_6$ is a particularly exciting representative of this exclusive class. The compound was discovered quite a while ago [1,2], but $Ca_3Co_2O_6$ long remained unnoticed and the interest first took off after the crystal and co-operative magnetic structures had been clarified [3,4]. Then it became clear that $Ca_3Co_2O_6$ takes a quasi-one-dimensional crystal structure (Fig. 1) with infinite Co_2O_6 chains running along the trigonal axis of a rhombohedral unit cell (space group $R\bar{3}c$), bonded together by intermediate Ca atoms. The structure of $Ca_3Co_2O_6$ is probably most correct described as of K_4CdCl_6 type, but references to other isotypic compounds, e.g., $Sr_3TT'O_6$ (T=Co, Ni, Cr, Zn; T'=Co, Ir, Pt), are frequently found in the literature.

An exotic feature with $Ca_3Co_2O_6$ is the alternate arrangement of crystallographically different Co atoms in octahedral (o; $Co1O_6^o$) and trigonal-prismatic (t; $Co2O_6^t$) environments along the chains.

There is general consensus that these distinct Co atoms carry differently sized magnetic moments that are subject to co-operative ordering at low temperature. Ever since the discovery of the appreciably different magnetic moments for $Co1^o$ and $Co2^t$ (0.08 ± 0.04 vs. $3.00 \pm 0.05\,\mu_B$, respectively [4]), attention has been focused on the valence states of these atoms. Aasland et al. [4] considered three possible interpretations (introducing the abbreviations LS = low spin and HS = high spin): (i) $Co1^o$ with Co^{III}, LS and $Co2^t$ with Co^{III}, HS, (ii) $Co1^o$ with Co^{IV}, LS and $Co2^t$ with Co^{II}, HS, and (iii) $Co1^o$ with a mixture of Co^{II}, LS and Co^{IV}, LS and $Co2^t$ with Co^{III}, HS. Alternative (iii) has not been tested neither experimentally nor theoretically.

Since these possibilities immediately appeared indistinguishable on the basis of magnetic property data alone (see Refs. [4,5]) several more or less parallel studies [6–11] have attempted to resolve the problem by electronic structure calculations. Broadly speaking Refs. [6,8–10] have favoured alternative (i) whereas Ref. [7] supported alternative (ii) (for reasons described in more detail in Ref. [11]).

*Corresponding author. Fax: +47 63 81 63 56.
E-mail address: Charles.Hervoches@ife.no (C.H. Hervoches).

0022-4596/$ - see front matter © 2006 Elsevier Inc. All rights reserved.
doi:10.1016/j.jssc.2006.10.037

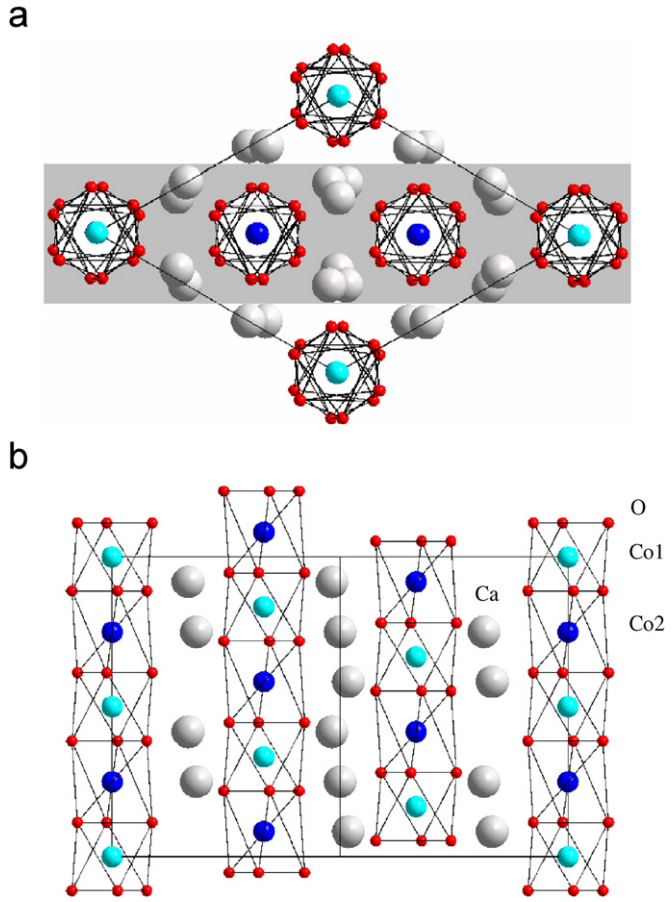

Fig. 1. The $Ca_3Co_2O_6$ structure: (a) projected along [001] and (b) as a section through the atomic arrangement covering the shaded field in part a. Legends for crystallographically different kinds of atoms are shown on the illustration.

It should be emphasized that Refs. [6–11] have used computer codes with quite different approximations for the density-functional-theory calculations and different valence-state indicators for interpretation of the results. This may explain part of the discrepancies. However, a part of the theory-based valence-state dispute probably trivially boils down to a difference in opinion on the use of the concepts valence state and oxidation state as synonyms (viz., in essence a mixed iono–covalent vs. a ionic picture of the bonding situation for Co in $Ca_3Co_2O_6$). According to the clarifications in Ref. [11] it appears that the discrepancy is now largely resolved in favor of alternative (i) with the valence state III for both $Co1^o$ and $Co2^t$.

Motivated by the disagreement on the interpretation of the theoretical findings, two very recent experimental studies have approached the valence-state problem. Both the ^{59}Co NMR examination [12] at 6–15 K and the X-ray photoemission spectroscopic investigation [13] at room temperature conclude that alternative (i) describes the valence states of $Ca_3Co_2O_6$. However, as will be advocated below the interpretations are not so unambiguous.

The magnetic data in Ref. [4] left behind open questions regarding transitions between different co-operative magnetic states. This aspect is later touched on in Refs. [6,8,14–21] without being fully resolved. However, the recent muon-spin-rotation and -relaxation technique study [21] has brought some clarification. The complex magnetic ordering process appears to start (not documented) with short-range one-dimensional ferromagnetic (F) configurations within the $(Co_2O_6)_\infty$ chains at ~200 K. This pattern develops further and is extended into short-range two-dimensional antiferromagnetic (AF) order below ~100 K (documented) which is converted into a long-range co-operative ferrimagnetic (Ferri) state at ~25 K, as also observed by neutron diffraction [4,5]. This ordering pattern appears, in turn, to be modified at lower temperature (see also Refs. [4,5,14,16,17]), but neither the exact nature of this (Ferri) state nor its origin is understood.

$Ca_3Co_2O_6$ exhibits interesting electric resistance and magneto-resistance phenomena which evidence a variable-range hopping mechanism with temperature-induced intrachain crossovers closely associated with the changes of magnetic state (see, e.g., Ref. [22]). However, conductivity properties as such are outside the scope of the present study.

This study focuses on substitutional solid-solution derivatives of $Ca_3Co_2O_6$ with rare-earth elements (R, including Y) on the Ca site and the effects on structure and magnetism of such substitution.

While this project has been in progress a few reports on $Ca_{3-v}R_vCo_2O_6$ (R=Y, La [19,23–25]) and $Ca_{3-v}Bi_vCo_2O_6$ [26] have appeared. Although these reports contain magnetic data, systematic attempts have not been made to clarify the valence-state and magneto-transition aspects mentioned above. This is, however, exactly the prime target of this paper. In addition, we report and discuss the solubility limits for the different substituents.

2. Experimental section

All samples were prepared from $CaCO_3$ (Merck, p.a.), $SrCO_3$ (Fluka, mass fraction >98%), $Co(CH_3COO)_2 \cdot 4H_2O$ (Fluka, mass fraction >99%), citric acid monohydrate $C_3H_4(OH)(COOH)_3 \cdot H_2O$ (Normann Prolabo, mass fraction >99.7%) and the appropriate rare-earth oxides (R_2O_3, R=Y, Pr, Nd, Sm, Eu, Gd, Tb, Dy, Ho, Yb, and Lu from Molycorp, Aldrich, Strem or Megon, all with mass fraction ⩾99.9%). The Co content of the acetate was determined gravimetrically.

Excess amount of citric acid was first mechanically mixed with the appropriate rare-earth oxide and then melted on a warm heating plate while adding a few droplets of distilled water in order to increase the heat conductivity and to avoid thermal decomposition of the acid. After complete dissolution of the oxide in the melt, 10–15 mL of distilled water was added together with $CaCO_3$ (and $SrCO_3$ for the $Ca_{3-v}Sr_vCo_2O_6$ specimens) and finally Co acetate under stirring. This mixture was heated on a hot plate at ~170 °C until a clear glassy gel had appeared.

The gel was dehydrated at 150 °C overnight, crushed, and incinerated at 450 °C for a few hours in order to remove carbonaceous species. The samples were then ground in an agate mortar and pressed into pellets, which were heated in alumina crucibles at 1000 °C for at least 1 week with intermediate grindings. All samples with $v > 0.9$ according to the formula $Ca_{3-v}R_vCo_2O_6$ proved to be phase impure and such samples were attempted re-annealed at increasingly higher temperature up to around 1200 °C which appears to be the decomposition temperature at the *R*-rich phase limit of $Ca_{3-v}R_vCo_2O_6$. Particular care was paid to equilibration of samples used for structure determination.

All samples were checked for phase purity and structurally characterized at room temperature by powder X-ray diffraction (PXD) using a Bruker AXS D-5000 X-ray diffractometer with monochromatic Cu$K\alpha_1$ radiation ($\lambda = 1.540598$ Å) and position sensitive detectors.

Powder neutron diffraction (PND) data were collected with the high-resolution powder neutron diffractometer PUS [27] at the JEEP II reactor, Kjeller, Norway. Cylindrical vanadium sample holders were used. Monochromatic neutrons with wavelength $\lambda = 1.5554$ Å were obtained from a Ge(511) focusing monochromator. The detector unit consists of two banks of seven position-sensitive ^{3}He detectors, each covering 20° in 2θ. Intensity data were collected from $2\theta = 10$–130° in steps of $\Delta(2\theta) = 0.05°$. Temperatures between 7 and 298 K were obtained by means of a Displex cooling system. A Lake Shore DRC 82C controller was used, and the temperature was measured and controlled by means of a silicon diode. Structure determination and profile refinement were performed using the Rietveld refinement programme Fullprof.98 [28]. Fig. 2 shows the fit between observed and calculated PND profiles obtained for $Ca_{2.25}Y_{0.75}Co_2O_6$ as a typical example of the good agreements generally obtained in this study ($R_p = 0.121$, $R_{wp} = 0.123$, $R_{exp} = 0.127$, and $\chi^2 = 0.936$ for $Ca_{2.25}Y_{0.75}Co_2O_6$). Neutron scattering lengths and magnetic form factors were taken from the program library.

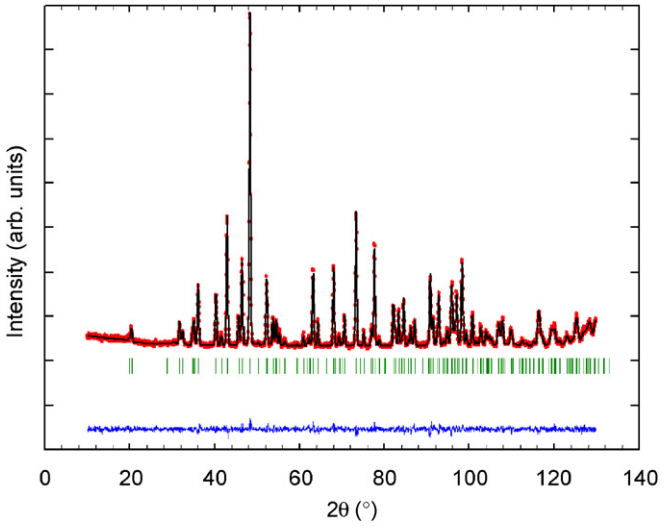

Fig. 2. Observed (points), calculated (tracing), and difference (lower profile; on the same scale) powder neutron diffraction (PND) pattern for $Ca_{2.25}Y_{0.75}Co_2O_6$ at 298 K. Vertical bars indicate the location of reflections.

Magnetic susceptibility data were recorded in zero-field-cooled (ZFC) mode with an MPMS magnetometer (Quantum Design) between 5 and 300 K for applied magnetic fields (H) from 25 to 1000 Oe. Field-cooled (FC) experiments were performed for $H = 1$ kOe. Magnetization data at 5 K were recorded for fields up to 50 kOe. Saturation magnetization was estimated by $1/H$ extrapolation.

3. Results and discussion

3.1. Solid solubility and structural features

It is convenient to first present the findings for $Ca_{3-v}Y_vCo_2O_6$ since this phase carries virtually all characteristics of the $Ca_{3-v}R_vCo_2O_6$ series. As seen from Fig. 3 the solid solubility extends up to a two-phase region at $v = 0.90 \pm 0.01$. Despite numerous attempts with variation of the equilibration conditions (see Experimental section) it proved impossible to extend the phase beyond the said limit.

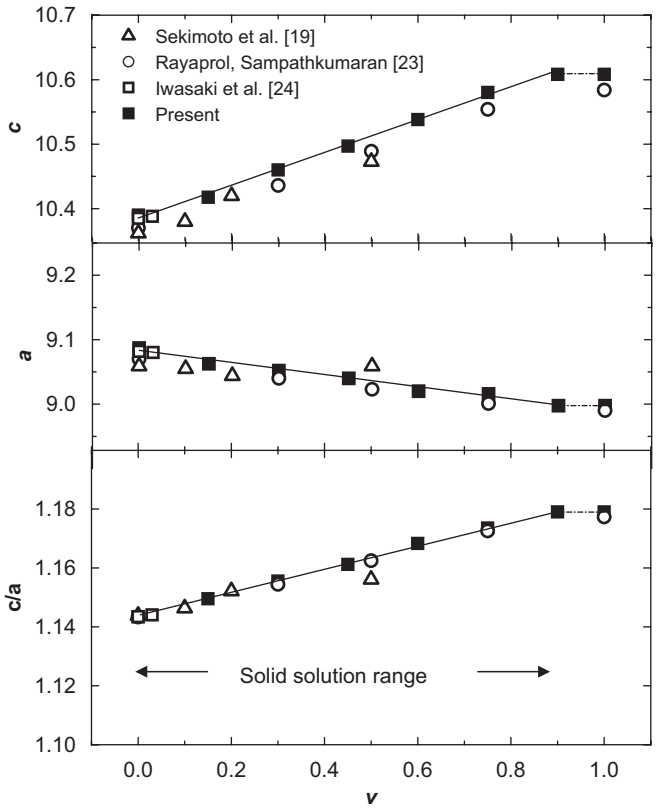

Fig. 3. Unit-cell dimensions (in Å) and c/a ratio as function as yttrium content (v) in $Ca_{3-v}Y_vCo_2O_6$. References to data quoted from other studies are given on the illustration. Lines are guides for eye.

The unit-cell dimensions (a and c as well as c/a and volume) vary approximately linearly with the substitution parameter v. The agreement with earlier studies [19,23,24] is acceptable when differences in synthesis and characterization procedures are taken into account.

Atomic co-ordinates were determined by profile refinements of PND data for the $Ca_{3-v}Y_vCo_2O_6$ samples with $v = 0.30$, 0.75, and 0.90. The derived unit-cell dimensions and atomic co-ordinates for $Ca_{3-v}Y_vCo_2O_6$ are included in Table 1. The patterns in Fig. 2 along with the low values for the calculated standard deviations prove a successful fitting. Despite that all atomic co-ordinates for the $Ca_{3-v}Y_vCo_2O_6$ phase change fairly regularly with v we suggest that these parameters, to a reasonable first approximation, should be regarded as invariant. The numerical changes are small and the calculated standard deviations almost certainly give overoptimistic impressions of the actual accuracy. Nevertheless, note that good fits between observed and calculated PND profiles along with systematic variations in the structural parameters (see also below) provide evidence for the postulated formula $Ca_{3-v}Y_vCo_2O_6$, i.e., there are no significant amount of oxygen defects. Separate analyses of the oxygen contents were therefore not considered necessary.

The variations in the most interesting interatomic distances $Co1^o$–O, $Co2^t$–O, and $Co1^o$–$Co2^t$ with the degree of substitution v (Fig. 4) show that the $Co1^o$–O distance remains virtually unchanged within the experimental error limit whereas the $Co2^t$–O and $Co1^o$–$Co2^t$ distances have increased by some 5% at the phase boundary. Hence, the replacement of Ca by Y has in addition to an effect on lattice dimensions (see Fig. 3), also an effect on the size of $Co2^t$.

Table 1
Unit-cell dimensions (in Å; volume in Å^3) and atomic coordinates for $Ca_{3-v}R_vCo_2O_6$ with $v = 0.30$ (calculated standard deviation in parenthesis), including corresponding data for a few other compositions (specified in footnotes)

R	a	c	V	x(Ca/R)	x(O)	y(O)	z(O)
Data collected at 298 K							
Ca[a]	9.0793(7)	10.381(1)	741.1(1)	0.3690(2)	0.1767(2)	0.0238(2)	0.1138(1)
Sr[b]	9.104(1)	10.397(1)	746.4(1)	—	—	—	—
Sr[c]	9.1211(7)	10.4100(5)	750.0(1)	0.3673(4)	0.1757(3)	0.0242(3)	0.1138(2)
Y[d]	9.062(1)	10.418(1)	741.0(1)	—	—	—	—
Y[e]	9.052(1)	10.460(1)	742.2(1)	0.3684(3)	0.1780(2)	0.0236(3)	0.1122(2)
Y[f]	9.040(1)	10.497(1)	742.9(1)	—	—	—	—
Y[g]	9.020(1)	10.538(1)	742.5(1)	—	—	—	—
Y[h]	9.0157(2)	10.5802(3)	744.8(1)	0.3673(4)	0.1802(4)	0.0244(4)	0.1104(2)
Y[i]	8.9975(1)	10.6083(2)	743.7(1)	0.3666(2)	0.1808(1)	0.0242(1)	0.1097(1)
Pr	9.0973(4)	10.4907(3)	751.8(1)	0.3676(2)	0.1768(1)	0.0244(1)	0.1123(1)
Nd	9.0932(4)	10.4891(3)	751.1(1)	0.3683(3)	0.1768(2)	0.0241(2)	0.1117(1)
Sm	9.079(1)	10.475(1)	747.8(1)	—	—	—	—
Eu	9.073(1)	10.475(1)	746.8(1)	—	—	—	—
Gd	9.066(1)	10.467(1)	745.0(1)	—	—	—	—
Tb	9.0621(4)	10.4678(3)	744.5(1)	0.3678(2)	0.1776(2)	0.0245(2)	0.1124(1)
Dy	9.056(1)	10.467(1)	743.4(1)	—	—	—	—
Ho	9.0560(3)	10.4663(2)	743.3(1)	0.3675(2)	0.1781(1)	0.0246(1)	0.1121(1)
Yb	9.0385(7)	10.4515(6)	739.4(1)	0.3675(4)	0.1783(3)	0.0245(3)	0.1122(2)
Lu	9.040(1)	10.453(1)	739.8(1)	—	—	—	—
Data collected at 7–10 K							
Ca[a]	9.060(1)	10.366(1)	736.9(2)	0.3705(4)	0.1770(2)	0.0233(3)	0.1142(2)
Y[e]	9.0350(8)	10.4425(9)	738.2(1)	0.3684(3)	0.1785(2)	0.0243(3)	0.1124(2)
Y[h]	8.9938(9)	10.557(1)	739.5(1)	0.3681(4)	0.1806(4)	0.0251(4)	0.1103(2)
Pr	9.0765(3)	10.4712(2)	747.1(1)	0.3680(2)	0.17735(9)	0.0242(1)	0.11231(7)
Nd	9.0735(4)	10.4718(3)	746.6(1)	0.3678(3)	0.1771(2)	0.0245(2)	0.1123(1)
Tb	9.0376(4)	10.4413(3)	738.6(1)	0.3681(2)	0.1780(1)	0.0245(1)	0.11230(9)
Ho	9.0296(3)	10.4401(5)	737.2(1)	0.3681(3)	0.1780(2)	0.0242(2)	0.1124(1)
Yb	9.0228(6)	10.4360(5)	735.8(1)	0.3678(3)	0.1794(2)	0.0254(2)	0.1125(2)

Space group $R\bar{3}c$ (hexagonal setting) with $Co1^o$ in 6*b* (0,0,0), $Co2^t$ in 6*a* (0,0,$\frac{1}{4}$), etc., Ca/R in 18*e* (x,0,$\frac{1}{4}$), etc., and O in 36*f* (x,y,z), etc.

[a] $Ca_3Co_2O_6$; data quoted from Refs. [3,4]; reference phase.

[b] $Ca_{2.85}Sr_{0.15}Co_2O_6$.

[c] $Ca_{2.70}Sr_{0.30}Co_2O_6$.

[d] $Ca_{2.85}Y_{0.15}Co_2O_6$.

[e] $Ca_{2.70}Y_{0.30}Co_2O_6$.

[f] $Ca_{2.55}Y_{0.45}Co_2O_6$.

[g] $Ca_{2.40}Y_{0.60}Co_2O_6$.

[h] $Ca_{2.25}Y_{0.75}Co_2O_6$.

[i] $Ca_{2.10}Y_{0.90}Co_2O_6$.

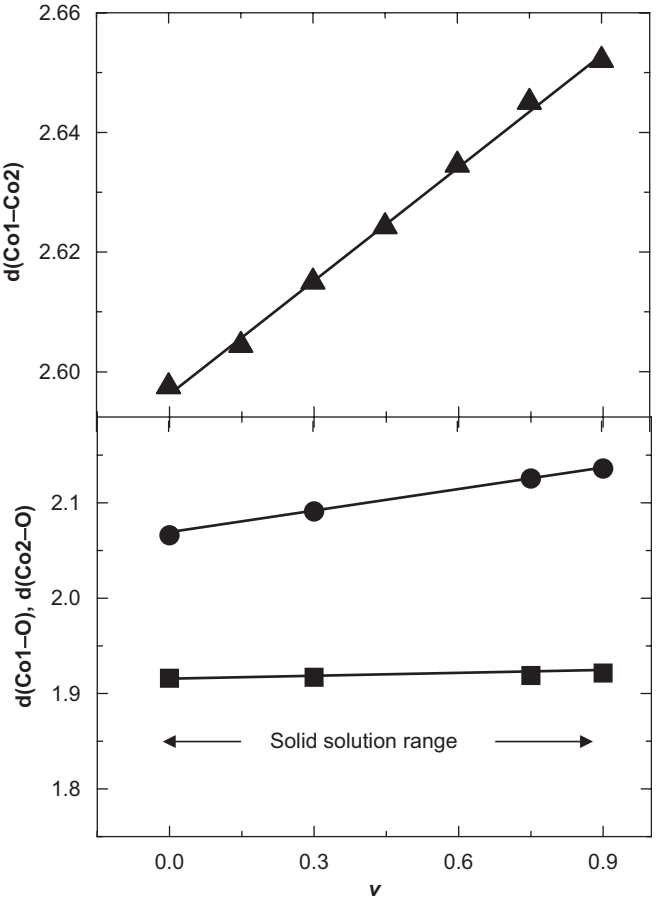

Fig. 4. Variation in interatomic distances (in Å; $Co1^{o}$–O (octahedral co-ordination), $Co2^{t}$–O (trigonal prismatic co-ordination), and $Co1^{o}$–$Co2^{t}$) with Y content in $Ca_{3-v}Y_vCo_2O_6$. The lines are generated from the linear relationships for a and c in Fig. 2, assuming invariant atomic co-ordinates for all sites in $Ca_{3-v}Y_vCo_2O_6$. The points refer to actual structural parameters given in Table 1. Lines are guides for eye.

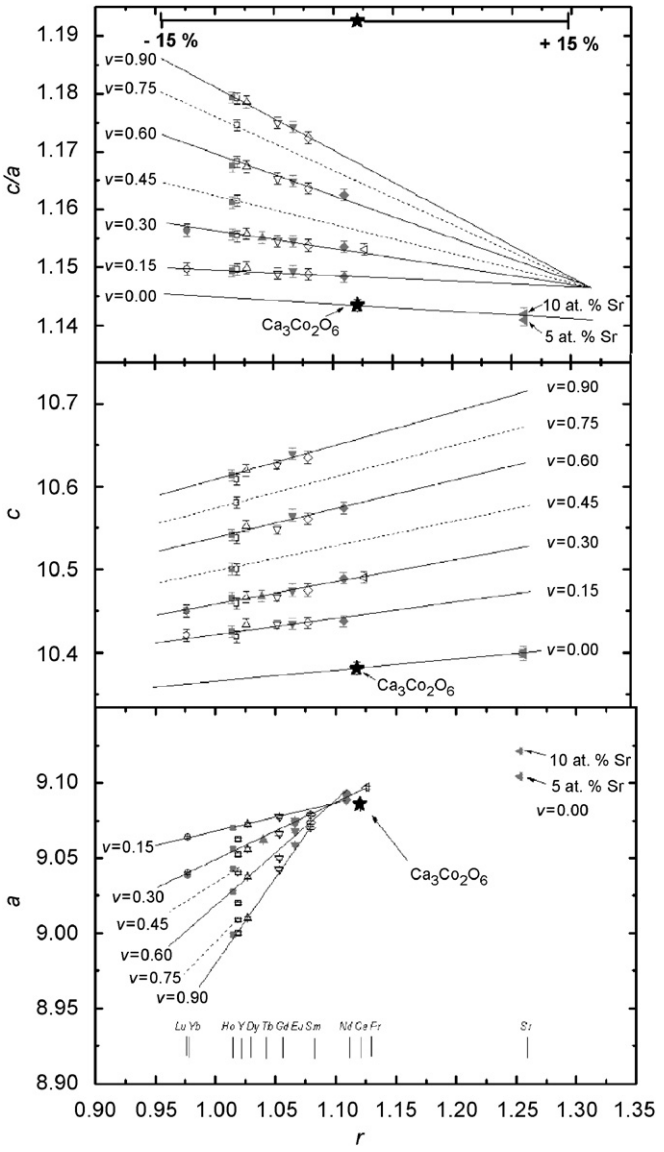

Fig. 5. Unit-cell dimensions (in Å) and c/a ratio as a function of the ionic radius of R (r standard value in Å) for $Ca_{3-v}R_vCo_2O_6$. Data for $Ca_{3-v}Sr_vCo_2O_6$ are included for comparison. Lines are guides for eye.

These observations are furthermore supported by the structural data for the $Ca_{3-v}R_vCo_2O_6$ series in Figs. 5 and 6. As seen from Fig. 5 the a axis is ruled by the size of R and the substitution level v. The very fact that a correlates with the standard ionic radius (r) of the R constituents (and Sr for $Ca_{3-v}Sr_vCo_2O_6$ with $v = 0.15$ and 0.30, marked as 5 and 10 at% in Fig. 5) shows that the substituents enter the Ca sublattices with their characteristic size. However, a different relationship exists between c and r, see Fig. 5. This clearly conveys that an additional size parameter must be in operation. This feature originates from an increasing size of $Co2^{t}$ with increasing v, and is easily recognized from the plots of the interatomic distances $Co1^{o}$–O, $Co2^{t}$–O, and $Co1^{o}$–$Co2^{t}$ in Fig. 6. $Co1^{o}$–O is virtually invariant for the entire $Ca_{3-v}R_vCo_2O_6$ series whereas $Co2^{t}$–O and $Co1^{o}$–$Co2^{t}$ clearly depend on both v and R. The extensive solid solubility of R in $Ca_3Co_2O_6$ is in accordance with the empirical 15%-size rule of Hume-Rothery [29] (see Figs. 5 and 6). The solid-solubility limit is found at $v \approx 0.90$ in all cases tested in this study. We have no explanation to offer as to why $v \approx 0.90$ constitutes the solubility limit rather than $v = 1.00$ (viz. $Ca_2RCo_2O_6$).

On the basis of the structural findings it seems justified to claim that the solutes R are randomly distributed over the Ca sublattice as $3+$ ions (documented by Fig. 5). The extra electrons provided by the R constituents are considered transferred to the $Co2O_6^t$ units of the $(Co_2O_6)_\infty$ chains (changes in oxygen stoichiometry are, as already mentioned, ruled out). Owing to the polar covalent character of the bonding within the $(Co_2O_6)_\infty$ chains it is difficult to estimate the actual charge associated with $Co1^{o}$, $Co2^{t}$, and O (see Ref. [11]). Nevertheless, the introduction of the higher valent Y^{3+} for Ca^{2+}, is best considered to be accompanied by a lowering of the valence state of $Co2^{t}$ from III toward II in the $Co2O_6^t$ units. It is likely that the

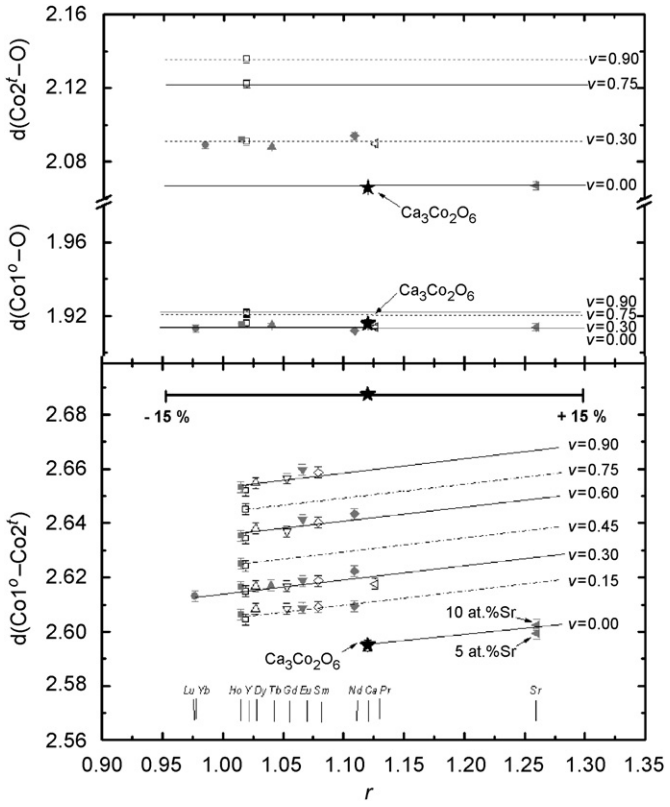

Fig. 6. Interatomic distances (in Å) $Co1^o$–O, $Co2^t$–O and $Co1^o$–$Co2^t$ as function of the ionic radius of R (r, standard values in Å). Data for $Ca_{3-v}Y_vCo_2O_6$ are included for comparison. Lines are guides for eye.

$Co1^o$ state is retained as a III, LS state in the solid-solution phase. These findings are to some extent supported by bond-valence [30] considerations. The bond-valence sum for $Co1^o$ remains ~3.2 independent of v whereas that for $Co2^t$ decreases form ~2.2 for $v=0$ to ~1.9 for $v=0.90$. (Note that the bond-valence radii for Co are somewhat uncertain, in particular for Co^{III}, and the well-documented size variations with spin state are not taken into account in the tabulated [30] bond-valence parameters.)

3.2. Magnetic properties

The temperature dependence of the magnetic susceptibility of $Ca_{3-v}Y_vCo_2O_6$ shows a slight systematic deviation from Curie–Weiss-law behaviour, below ~200 K for samples with $0<v<\sim0.3$. (Fig. 7 only shows the more interesting χ^{-1} characteristics below 100 K but see also Fig. 8.) At around 20 K, dents on the curves evidence that new magnetic phenomena set in. Together with similar findings for $Ca_{3-v}R_vCo_2O_6$ (Fig. 8) these observations support the claimed many-stage magnetic-ordering process from short-range one-dimensional F via intermediate AF patterns to long-range three-dimensional Ferri order. The temperature for the onset of the long-range three-dimensional Ferri order is established at ~25 K for $v=0$, however, it decreases rapidly (see Table 2 and Fig. 8) with increasing R content.

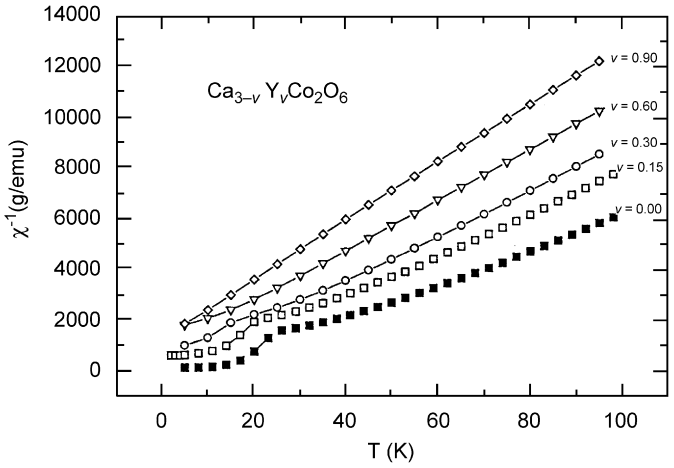

Fig. 7. Reciprocal magnetic susceptibility ($H=1$ kOe) vs. temperature for $Ca_{3-v}Y_vCo_2O_6$. Effective magnetic moment (μ_{eff} in μ_B), Weiss constant (θ in K), and co-operative ordering temperature (T_c in K) for these samples are according to increasing v: 5.5(1), 31, 24; 5.3(1), 18, 20; 5.1(1), 15, 13; 5.1(1), 9, –; 5.0(1), –6, –.

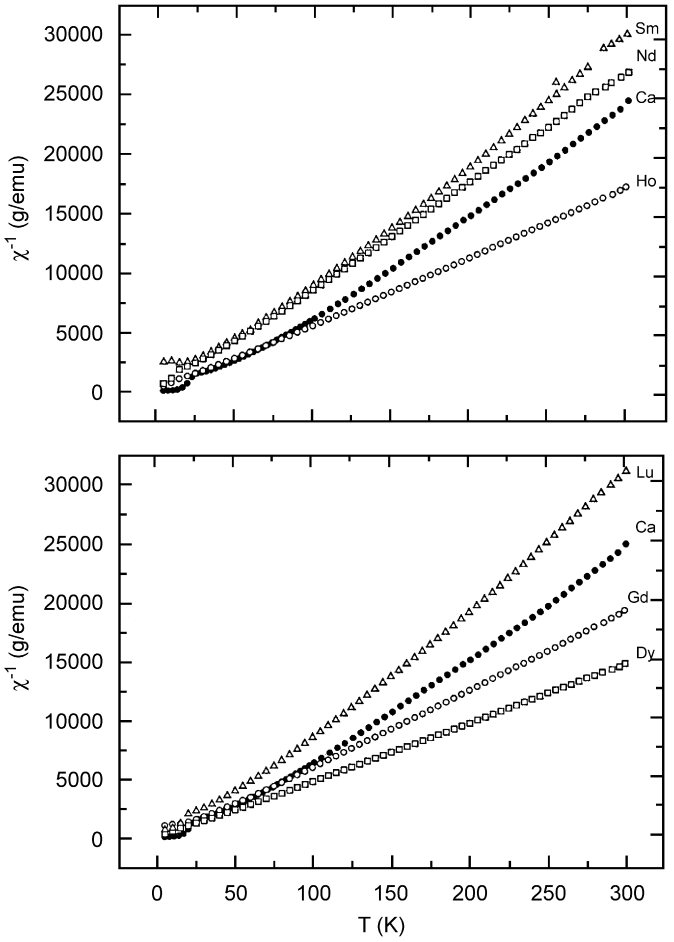

Fig. 8. Reciprocal magnetic susceptibility ($H=1$ kOe) vs. temperature for $Ca_{2.70}R_{0.30}Co_2O_6$ for various rare-earth solutes (see the labels on the illustration).

There are just vague indications in the magnetic susceptibility for magnetic order for an Y content of $v\geq0.3$. However, as seen from Fig. 9, for $Ca_{2.70}Y_{0.30}Co_2O_6$

Table 2
Magnetic data for $Ca_{2.70}R_{0.30}Co_2O_6$: Effective paramagnetic moment (μ_p), Weiss constant (θ), and co-operative magnetic ordering temperature according to dent (T_{dent}) on inverse magnetic susceptibility curve together with co-operative magnetic moments for Co1^o and Co2^t (along c) as refined from PND data (calculated standard deviation in parenthesis) recorded at at 7–10 K ($T_{meas.}$)

R	μ_p (μ_B)	θ (K)	T_{dent} (K)	M_c;Co1 (μ_B)	M_c;Co2 (μ_B)	$T_{meas.}$ (K)
Ca[a]	5.5	31	24	0.03(4)	2.96(5)	10
Sr[b]		23	24	—	—	—
Sr[c]	5.1	26	24	—	—	—
Y[d]	5.3	18	20	—	—	—
Y[e]	5.1	15	13	0.15(4)	2.41(4)	10
Y[f]	5.1	4	—	—	—	—
Y[g]	5.0	−6	—	—	—	—
Pr	5.2	12	14	0.12(3)	2.74(4)	8
Nd	5.3	10	14	−0.02(7)	2.64(8)	7
Sm	5.2	26	12	—	—	—
Eu	5.2	7	15	—	—	—
Gd	5.1	8	—	—	—	—
Tb		4	14	0.06(6)	2.69(7)	8
Dy	5.1	4	—	—	—	—
Ho	4.1	4	13	−0.02(6)	2.69(7)	8
Yb	—	—	—	0.29(15)	1.73(16)	8
Lu	5.2	25	20	—	—	—

[a]$Ca_3Co_2O_6$; data quoted from Ref. [4]; reference phase.
[b]$Ca_{2.85}Sr_{0.15}Co_2O_6$.
[c]$Ca_{2.70}Sr_{0.30}Co_2O_6$.
[d]$Ca_{2.85}Y_{0.15}Co_2O_6$.
[e]$Ca_{2.70}Y_{0.30}Co_2O_6$.
[f]$Ca_{2.40}Y_{0.60}Co_2O_6$.
[g]$Ca_{2.10}Y_{0.90}Co_2O_6$.

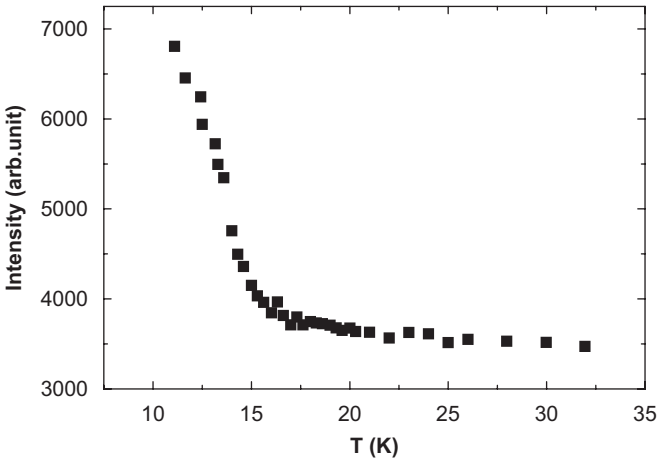

Fig. 9. Temperature dependence of integrated intensity of (100) Ferri peak for $Ca_{2.7}Y_{0.3}Co_2O_6$. $T_{ferri} = 15(1)$ K.

the appearance of PND reflections of Ferri origin proves an ordered magnetic state at ~15 K. Quite similar findings are obtained for the $Ca_{3-v}R_vCo_2O_6$ series as a whole. For some R-substituents, the magnetic-order process appears to extend beyond $v \approx 0.3$. However, for $Ca_{2.25}Y_{0.75}Co_2O_6$, PND shows no indication of magnetic order at 10 K.

The $M(H)$ curves in Fig. 10 show a tendency toward saturation of the Ferri state (↑↑↓ chain arrangements). For $H > 25$–35 kOe, a spin conversion to an F state is indicated (↑↑↑). The calculated effective paramagnetic moment decreases from 5.5 μ_B for $Ca_3Co_2O_6$ to 5.0 μ_B for

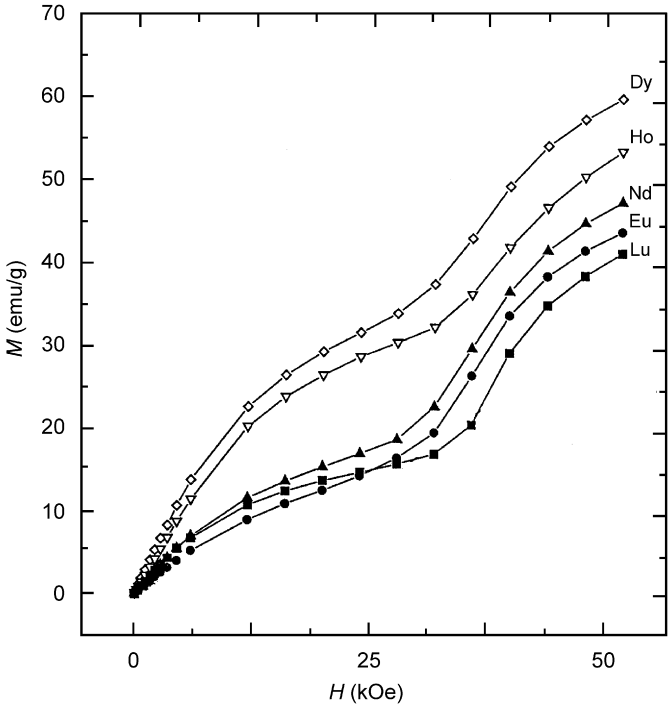

Fig. 10. Magnetization (M) vs. magnetic field (H) recorded at 5 K for $Ca_{2.70}R_{0.30}Co_2O_6$. The labelling for the R constituents is marked on the illustration.

$Ca_{2.1}Y_{0.9}Co_2O_6$, which also gives some supports to the claimed lowering of the valence state of Co2^t. The ordered magnetic moment as seen by PND decreases similarly

(Table 2), in qualitative accordance with the anticipated Co^{III} to Co^{II} conversion. Thus, the transfer of electrons to the $Co2^t$ sites diminishes both the magnetic moment of $Co2^t$ and the co-operative magnetic transition temperature. However, the reduction of the magnetic moment is smaller than expected and the disappearance of the co-operative magnetic state occurs earlier than expected. There are many factors which may influence the magnetic situation in such phases. Many of the *R* substituents carry a magnetic moment of their own but it is not easy to see how this feature can influence the co-operative state for the Co sublattices. The degree of electron delocalization within the $Co1^o$–$Co2^t$ chains is clearly of great importance for the properties of the co-operative magnetic state. The covalent character of the Co–O bonds is another feature which may turn out to be of great importance for the co-operative magnetic state.

In conclusion, both the crystallographic and magnetic data support the claim that R^{3+} substitution for Ca^{2+} leads to reduction of the magnetic moment of cobalt in the trigonal prismatic sites. However, the $Ca_{3-v}R_vCo_2O_6$ phases are clearly very rich in magnetically exciting properties and the present study really only represent a first course survey of magnetic consequences of *R*-for-Ca substitution in $Ca_3Co_2O_6$.

Acknowledgment

This work has received support from The Research Council of Norway, Grant 158518/431 (NANOMAT).

References

[1] C. Bisch, P. Rolando, Ann. Chim. (Rome) 58 (1968) 676.
[2] E. Woermann, A. Muan, J. Inorg. Nucl. Chem. 32 (1970) 1455.
[3] H. Fjellvåg, E. Gulbrandsen, S. Aasland, A. Olsen, B.C. Hauback, J. Solid State Chem. 124 (1996) 190.
[4] S. Aasland, H. Fjellvåg, B. Hauback, Solid State Commun. 101 (1997) 187.
[5] H. Kageyama, K. Yoshimura, K. Kosuge, H. Mitamura, T. Goto, J. Phys. Soc. Japan 66 (1997) 1607;
H. Kageyama, K. Yoshimura, K. Kosuge, X. Xu, S. Kawano, J. Phys. Soc. Japan 67 (1998) 357.
[6] M.-H. Whangbo, D. Dai, H.-J. Koo, S. Jobic, Solid State Commun. 125 (2003) 413;
A. Villesuzanne, M.-H. Whangbo, Inorg. Chem. 44 (2005) 6339.
[7] R. Vidya, P. Ravindran, H. Fjellvåg, A. Kjekshus, O. Eriksson, Phys. Rev. Lett. 91 (2003) 186404.
[8] V. Eyert, C. Lashinger, T. Kopp, R. Frésard, Chem. Phys. Lett. 385 (2004) 249.
[9] J. An, C.-W. Nan, Solid State Commun. 129 (2004) 51.
[10] H. Wu, M.W. Haverkort, Z. Hu, D.I. Khomskii, L.H. Tjeng, Phys. Rev. Lett. 95 (2005) 186401.
[11] R. Vidya, P. Ravindran, H. Fjellvåg, A. Kjeskhus, Phys. Rev. B submitted for publication.
[12] E.V. Sampathkumaran, N. Fujiwara, S. Rayaprol, P.K. Madhu, Y. Uwatoko, Phys. Rev. B 70 (2004) 014437.
[13] K. Takubo, T. Mizokawa, S. Hirata, J.-Y. Son, A. Fujimori, D. Topwal, D.D. Sarma, S. Rayaprol, E.V. Sampathkumaran, Phys. Rev. B 71 (2005) 073406.
[14] A. Maignan, C. Michel, A.C. Masset, C. Martin, B. Raveau, Eur. Phys. J. B 15 (2000) 657.
[15] B. Martinez, V. Laukhin, M. Hernando, J. Fontcuberta, M. Parras, J.M. Gonzales-Calbet, Phys. Rev. B 64 (2001) 012417.
[16] S. Niitaka, K. Yoshimura, K. Kosuge, M. Nishi, K. Kakurai, Phys. Rev. Lett. 87 (2001) 177202.
[17] V. Hardy, S. Lambert, M.R. Lees, D.M. Paul, Phys. Rev. B 68 (2003) 014424;
A. Maignan, V. Hardy, S. Hébert, M. Drillon, M.R. Lees, O. Petrenko, D.M. Paul, D. Khomskii, J. Mater. Chem. 14 (2004) 1231;
V. Hardy, D. Flahaut, M.R. Lees, O.A. Petrenko, Phys. Rev. B 70 (2004) 214439;
D. Flahaut, A. Maignan, S. Hébert, C. Martin, R. Retoux, V. Hardy, Phys. Rev. B 70 (2004) 094418.
[18] C. Lashinger, T. Kopp, V. Eyert, R. Frésard, J. Magn. Magn. Mater. 272–276 (2004) 974;
R. Frésard, C. Lashinger, T. Kopp, V. Eyert, Phys. Rev. B 69 (2004) 140405(R).
[19] T. Sekimoto, S. Noguchi, T. Ishida, J. Phys. Soc. Japan 73 (2004) 3217.
[20] D. Dai, M.-H. Whangbo, Inorg. Chem. 44 (2005) 4407.
[21] J. Sugiyama, H. Nozaki, J.H. Brewer, E.J. Ansaldo, T. Takami, H. Ikuta, U. Mizutani, Phys. Rev. B 72 (2005) 064418.
[22] B. Raquet, M.N. Baibich, J.M. Broto, H. Rakoto, S. Lambert, A. Maignan, Phys. Rev. B 65 (2002) 104442.
[23] K. Iwasaki, H. Yumane, S. Kubota, J. Takahashi, M. Shimada, J. Alloy Compd. 358 (2003) 210.
[24] S. Rayaprol, E.V. Sampathkumaran, Pramana 65 (2005) 491.
[25] C.H. Kim, K.H. Kim, S.H. Park, H.J. Paik, J.H. Cho, B.G. Kim, J. Phys. Soc. Japan 74 (2005) 2317.
[26] K. Iwasaki, H. Yamane, J. Takahashi, S. Kubota, T. Nagasaki, Y. Arita, Y. Nishi, T. Matsui, M. Shimada, J. Phys. Chem. Solids 66 (2005) 303.
[27] B.C. Hauback, H. Fjellvåg, O. Steinsvoll, K. Johansson, O.T. Buset, J. Jorgensen, J. Neutron Res. 8 (2000) 215.
[28] J. Rodriguez-Carvajal, T. Roisnel, International Union of Crystallography, Newsletter 20 (1998).
[29] W. Hume-Rothery, The Structure of Metals and Alloys, Institute of Metals, London, 1936.
[30] N.R. Brese, M. O'Keeffe, Acta Crystallogr., Sect. B 47 (1991) 192.